



SEISMIC PERFORMANCE OF BRIDGE COLUMNS WITH DOUBLE INTERLOCKING SPIRALS

Juan F. Correal¹, M. Saiid SAIIDI², David SANDERS³ and Saad El-AZAZY⁴

SUMMARY

Double or triple interlocking spirals as transverse reinforcement in bridge columns are being used especially in large rectangular cross sections not only because they provide more effective confinement than rectangular hoops but also because interlocking spirals make the column fabrication process easier. The behavior of columns with interlocking spirals has been studied only to a limited extent. A study is conducted at University of Nevada, on the seismic behavior of double interlocking spirals columns with funding by the California Department of Transportation (Caltrans).

This article presents the experimental study of two 1/4-scale columns with a low level of average shear stress ($3\sqrt{f'c}$) and four 1/5-scale columns with high level of shear stress ($7\sqrt{f'c}$), designed and constructed using current Caltrans details and procedures. All the columns had an oval shape and were tested under multiple amplitudes of Sylmar record using shake table simulation, in the strong direction of the columns. The spacing between center to center of the spirals (1.0 and 1.5 times R, the spiral radius) was the principal variable studied in the first four specimens. One of the remaining specimens had spacing between spirals equal to 1.25R and the other one had spacing between spirals equal to 1.5R with horizontal ties connecting the hoops. The shake table tests, for the first four specimens, showed that larger distance between the centers of the spirals (1.5 times the spiral radius) in columns with low level of average shear stress ($3\sqrt{f'c}$) did not lead to excessive shear cracking or a reduction of the shear capacity. In addition, displacement ductility capacity decreased when the level of average shear stress increased. Vertical cracks were observed within the interlocking region, in columns with larger distance between the centers of the spirals (1.5R) and high level of average shear stress ($7\sqrt{f'c}$). Horizontal cross ties connecting the hoops reduced vertical cracks in the interlocking region.

INTRODUCTION

The Seismic Design Criteria (SDC) of the California Department of Transportation (Caltrans) [1] is the only bridge code in The United States that provides specifications to design columns with interlocking spirals. Only a limited number of experimental and theoretical studies have been conducted on

¹ Ph.D Candidate, University of Nevada, Reno NV 89557, USA. Email: jcorreal@unr.edu

² Professor, University of Nevada, Reno NV 89557, USA. Email: saidi@unr.edu

³ Associate Professor, University of Nevada, Reno NV 89557, USA. Email: sanders@unr.edu

⁴ Senior Bridge Engineer, Caltrans, Sacramento, CA 95816-8041, USA. Email: saad_el_azazy@dot.ca.gov

interlocking spiral columns. Tanaka and Park (1993) [2], Buckingham (1993) [3], Benzoni (2000) [4] and Mizugami (2000) [5] studied the performance of columns with interlocking spirals. None of these studies included dynamic loading of the column using earthquake simulation on shake tables.

The objective of the research discussed in this article was to study the seismic performance of bridge columns with double interlocking spirals using the shake table simulations. The experimental results were used in order to determine if increasing of the distance between the centers of the spirals, d_i , affect the overall performance of the columns when they are subjected to different levels of average shear stress in function of $\sqrt{f'_c}$. A further objective was to verify if the adding of horizontal cross ties connecting the hoops can improve the overall performance of the column with d_i of 1.5 times the radius of spirals, R .

COLUMN DESIGN

Caltrans Provision

The SDC [1] denotes that a minimum element displacement ductility capacity of $\mu_c=3$ shall be specified for columns in ductile structures.

$$\mu_c = \frac{\Delta_c}{\Delta_{y^{col}}} \quad (1)$$

The member displacement capacity, Δ_c , is determined from moment-curvature ($M-\phi$) analysis with result idealized by an elasto-plastic relationship. $\Delta_{y^{col}}$ is the idealized effective yield displacement of the column. In the SDC [1], Δ_c of a cantilever member fixed at the base is defined as follows:

$$\Delta_c = \Delta_{y^{col}} + \Delta_p \quad (2)$$

where Δ_p is the idealized plastic displacement capacity due to rotation of the plastic hinge. $\Delta_{y^{col}}$ and Δ_p are defined in Eq. (3) and (4), respectively.

$$\Delta_{y^{col}} = \frac{L^2}{3} \phi_y \quad (3)$$

$$\Delta_p = \theta_p \left(L - \frac{L_p}{2} \right) \quad (4)$$

where L = distance from the point of maximum moment to the point of contra-flexure; ϕ_y = the idealized yield curvature defined by an elasto-plastic representation of the cross section $M-\phi$ curve; θ_p = plastic rotation capacity ($\theta_p = L_p \phi_p$); ϕ_p = idealized plastic curvature capacity ($\phi_p = \phi_u - \phi_y$); ϕ_u = curvature capacity at the failure limit state. L_p = equivalent analytical plastic hinge length is defined as:

$$L_p = 0.08L + 0.15f_{ye}d_{bl} > 0.3f_{ye}d_{bl} \quad (5)$$

where f_{ye} = expected yield stress for reinforcement; d_{bl} = nominal bar diameter of longitudinal column reinforcement.

Large-Scale Models

Two 1/4 scale columns with low level of average shear stress ($3\sqrt{f'_c}$) and four 1/5 scale columns with high level of average shear stress ($7\sqrt{f'_c}$) were constructed and designed using the SDC [1]. A target displacement ductility (μ_c) of 5 was selected. The average shear stress is defined as the maximum lateral force divide by 0.8 times the gross area and expressed as a function of $\sqrt{f'_c}$. The distance between the centers of adjacent spirals, d_i (1.0 and 1.5 times the radius of spirals, R) was the principal variable studied in the first four specimens. The spiral spacing in these columns is the lower and upper limit in Caltrans SDC [1]. One of the remaining specimens had a d_i of 1.25 times R and the other one had a d_i of 1.5 times R with horizontal cross ties connecting the hoops. The overall dimensions of the columns are shown in Figures 1 and 2. The specified concrete compressive strength of the columns was 34.5 Mpa (5000 psi) and the reinforcement was grade 60.

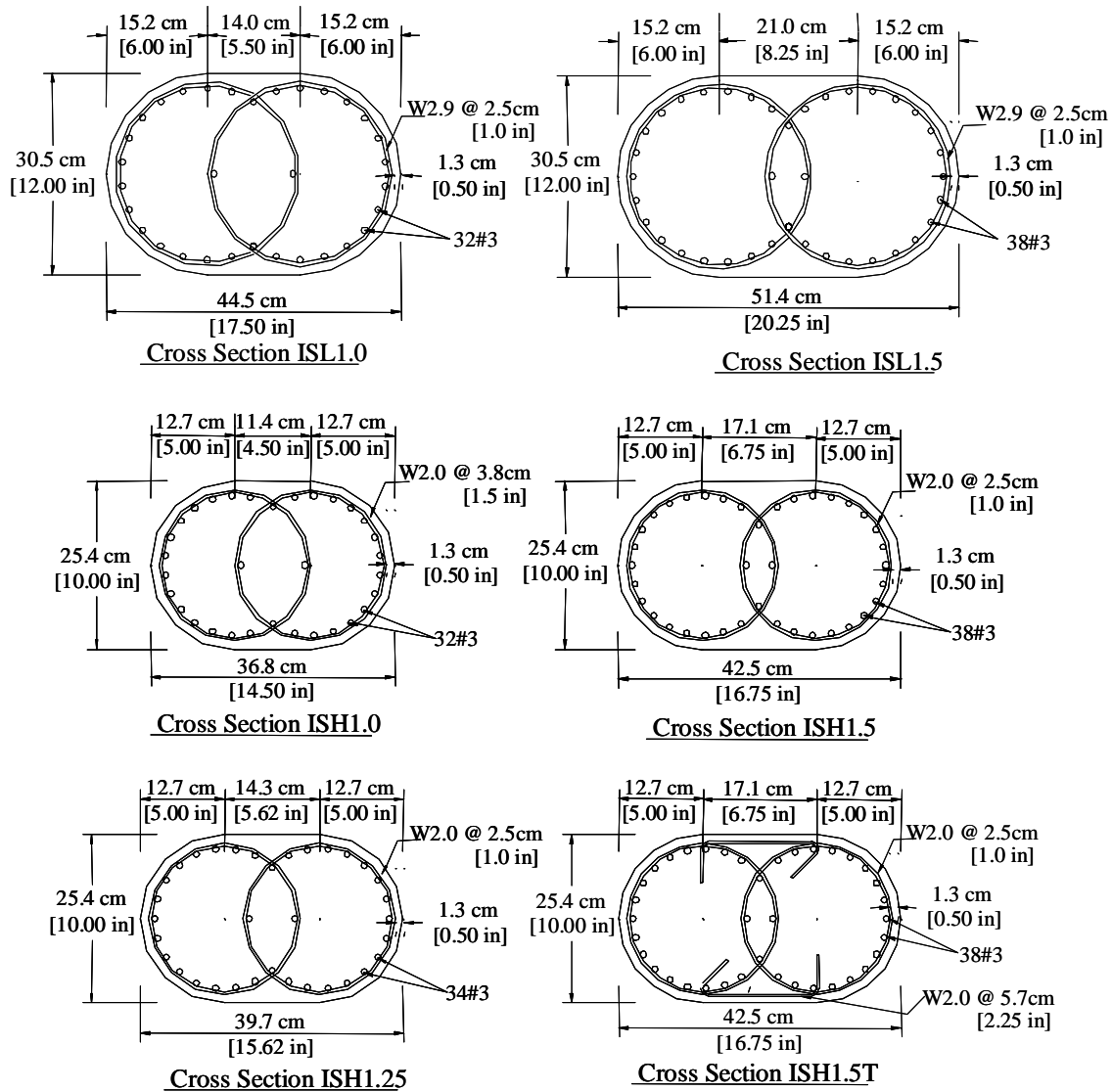


Figure 1. Test specimens cross section dimensions

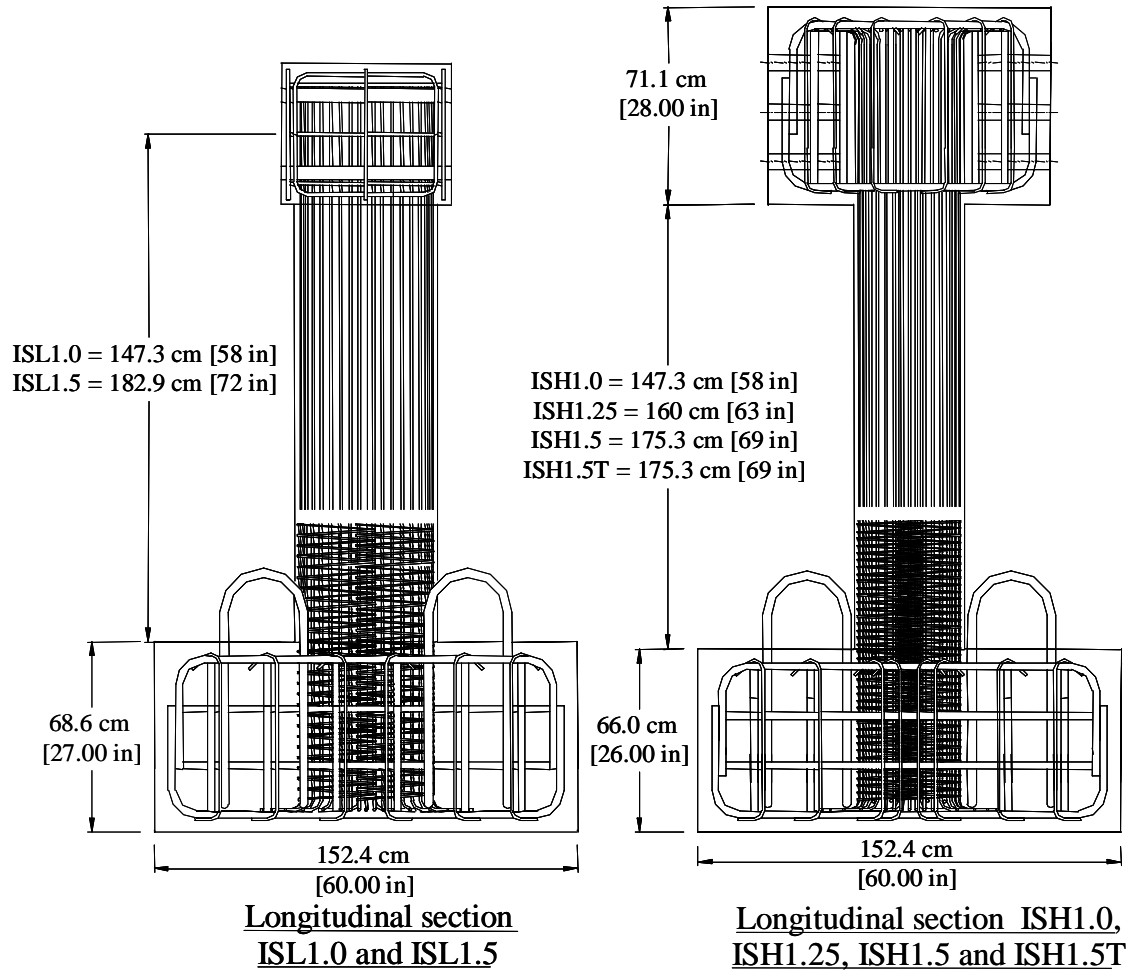


Figure 2. Test specimens elevations

TEST SETUP AND LOADING PROCEDURE

The test setup for single curvature and double curvature columns is shown in Figures 3 and 4, respectively. The test setup in single curvature was used in the specimens with low average shear stress (ISL1.0, ISL1.5) whereas the test setup in double curvature was used in the specimen with high average shear stress (ISH1.0, ISH1.25, ISH1.5 and ISH1.5T). The axial load of $0.1f'_cA_g$ was imposed through a steel spreader beam by prestressed bars to hydraulic jacks. The lateral load was applied through the inertial mass system off the table for better stability. Strain gages were used to measure the strains in the longitudinal and transverse steel. A series of curvature measurement instruments were installed in the plastic hinge zone. Displacement transducers forming panels were placed along the height of the column, in the test in double curvature, for measuring shear deformations. Load cells were used to measure both the axial and lateral forces. An additional measurement of the lateral force was taken by an accelerometer. Displacement transducers measured the lateral displacements of the columns.

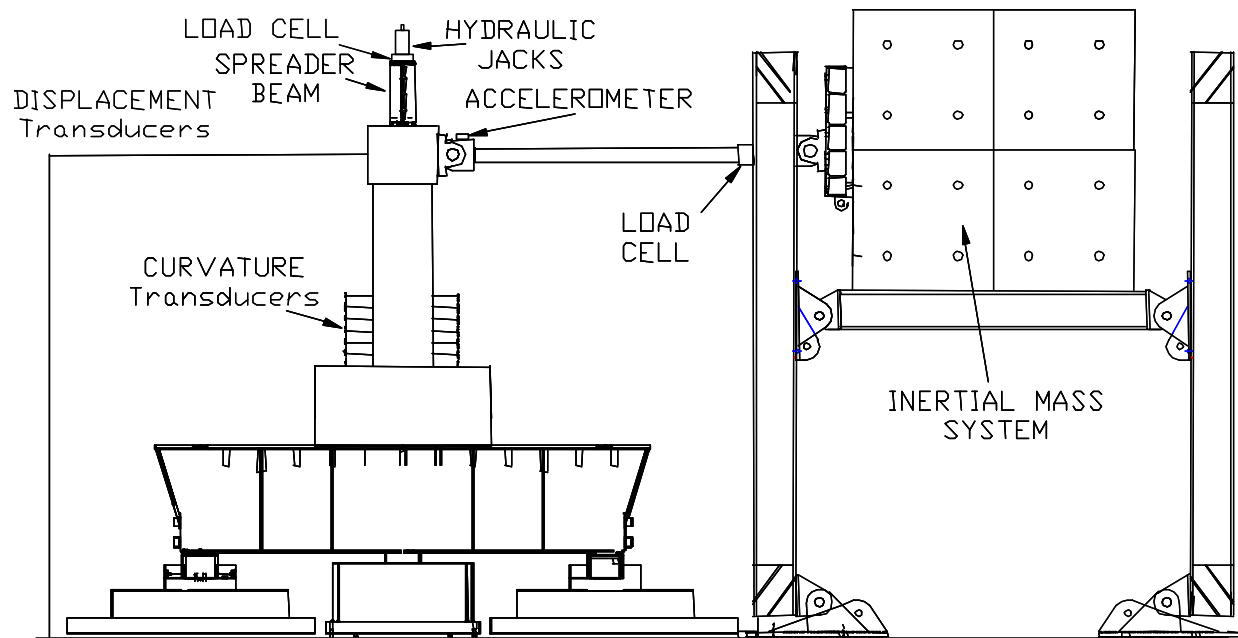


Figure 3. Single curvature test setup

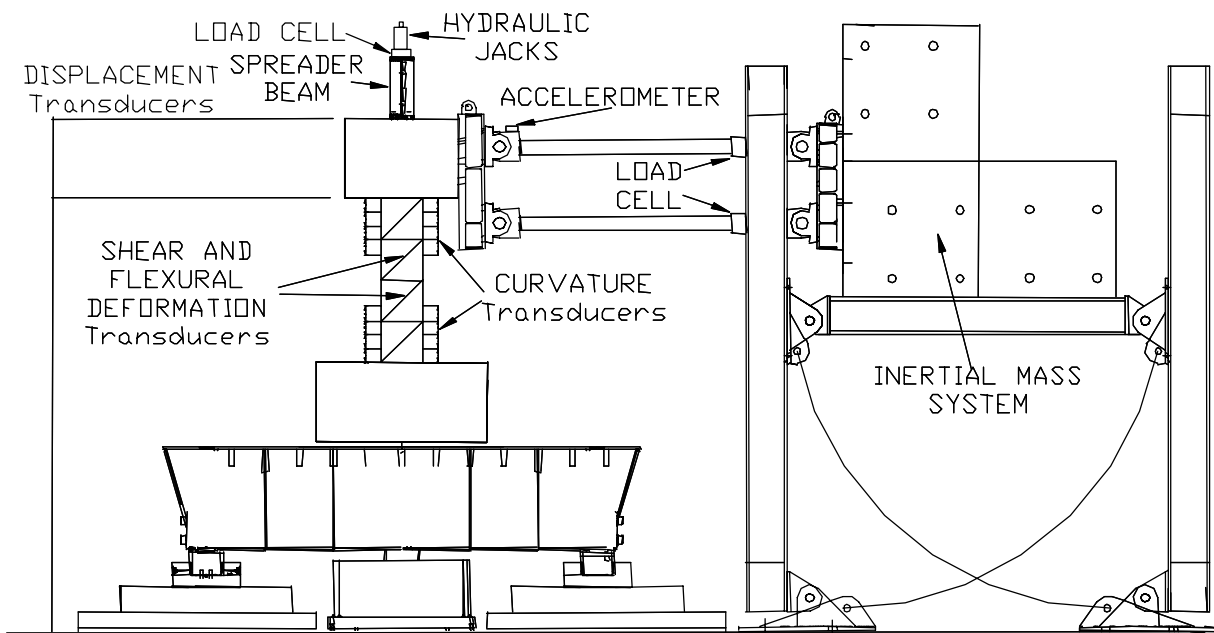


Figure 4. Double curvature test setup

Force and displacement capacity was calculated based on the plastic moment capacity of the columns from the $M-\phi$ analysis, using the program SPMC [6]. The idealized elasto-plastic force and displacement was used to perform a nonlinear response history analysis of the columns with program RCSake [7]. The

Sylmar record of the Northridge (0.606 g PGA), California 1994 earthquake, was selected as the input motion based on its high displacement ductility demand. The test motions are shown in Table 1. A time compression factor was applied to the original Sylmar record (30 seconds) in order to account for the scale factor of the models and adjustment due to inertia mass in specimens. Intermittent free vibration tests were conducted to measure the changes in frequency and damping ratio of the columns.

Table 1. Loading motions

| | Specimen | | | | | | | | | | | |
|-------|------------------------------|--------|-------------|---------|-------------|--------|-------------|---------|-------------|---------|-------------|---------|
| | ISL1.0 | | ISL1.5 | | ISH1.0 | | ISH1.25 | | ISH1.5 | | ISH1.5T | |
| | Time compression factor | | | | | | | | | | | |
| | 0.51 | | 0.50 | | 0.49 | | 0.46 | | 0.5 | | 0.45 | |
| | Target Acceleration [motion] | | | | | | | | | | | |
| Run # | g [xSlymar] | | g [xSlymar] | | g [xSlymar] | | g [xSlymar] | | g [xSlymar] | | g [xSlymar] | |
| 1 | 0.06 | [0.10] | 0.06 | [0.10] | 0.06 | [0.10] | 0.06 | [0.10] | 0.06 | [0.10] | 0.06 | [0.10] |
| 2 | 0.12 | [0.20] | 0.12 | [0.20] | 0.12 | [0.20] | 0.12 | [0.20] | 0.12 | [0.20] | 0.12 | [0.20] |
| 3 | 0.18 | [0.30] | 0.24 | [0.40] | 0.24 | [0.40] | 0.30 | [0.50] | 0.24 | [0.40] | 0.24 | [0.40] |
| 4 | 0.30 | [0.50] | 0.36 | [0.60] | 0.30 | [0.50] | 0.45 | [0.75] | 0.36 | [0.60] | 0.36 | [0.60] |
| 5 | 0.45 | [0.75] | 0.48 | [0.80] | 0.45 | [0.75] | 0.61 | [1.00] | 0.45 | [0.75] | 0.45 | [0.75] |
| 6 | 0.61 | [1.00] | 0.61 | [1.00] | 0.61 | [1.00] | 0.76 | [1.25] | 0.61 | [1.00] | 0.61 | [1.00] |
| 7 | 0.76 | [1.25] | 0.76 | [1.25] | 0.76 | [1.25] | 0.91 | [1.50] | 0.76 | [1.25] | 0.76 | [1.25] |
| 8 | 0.91 | [1.50] | 0.91 | [1.50] | 0.91 | [1.50] | 1.06 | [1.75] | 0.91 | [1.50] | 0.91 | [1.50] |
| 9 | 1.06 | [1.75] | 1.06 | [1.75] | 1.06 | [1.75] | 1.21 | [2.00] | 1.06 | [1.75] | 1.06 | [1.75] |
| 10 | 1.21 | [2.00] | 1.21 | [2.00] | 1.21 | [2.00] | 1.29 | [2.125] | 1.21 | [2.00] | 1.21 | [2.00] |
| 11 | | | 1.29 | [2.125] | | | 1.36 | [2.25] | 1.29 | [2.125] | 1.29 | [2.125] |
| 12 | | | | | | | 1.44 | [2.375] | 1.36 | [2.25] | 1.36 | [2.25] |
| 13 | | | | | | | | | 1.44 | [2.375] | 1.44 | [2.375] |
| 14 | | | | | | | | | | | 1.52 | [2.50] |
| 15 | | | | | | | | | | | 1.59 | [2.625] |

OBSERVED PERFORMANCE

Low Average Shear Stress Columns: ISL1.0 AND ISL1.5

Flexural cracks were observed in specimen ISL1.0 during the first three runs and in specimen ISL1.5 during the first six runs. First spalling and shear cracks were formed in specimen ISL1.0 at 0.5xSylmar and specimen ISL1.5 at 1.25xSylmar. Shear cracks were located in the interlocking region near to the lower portion of the column. Considerable spalling, as well as propagation of flexural and shear cracks was observed after 1.25xSylmar in specimen ISL1.0. At 1.5xSylmar and 1.75xSylmar spirals were visible in specimens ISL1.0 and ISL1.5, respectively. There was no visible core damage. Longitudinal bars were exposed after 1.75xSylmar in specimen ISL1.0. Specimens ISL1.0 and ISL1.5 (Figures 5 and 6) failed during 2.0xSylmar (1.21g PGA) and 2.125xSylmar (1.29g PGA), respectively. The failure in both columns was due to fracturing of the spirals and buckling of the longitudinal bars.



Figure 5. Specimens ISL1.0 after Collapse.

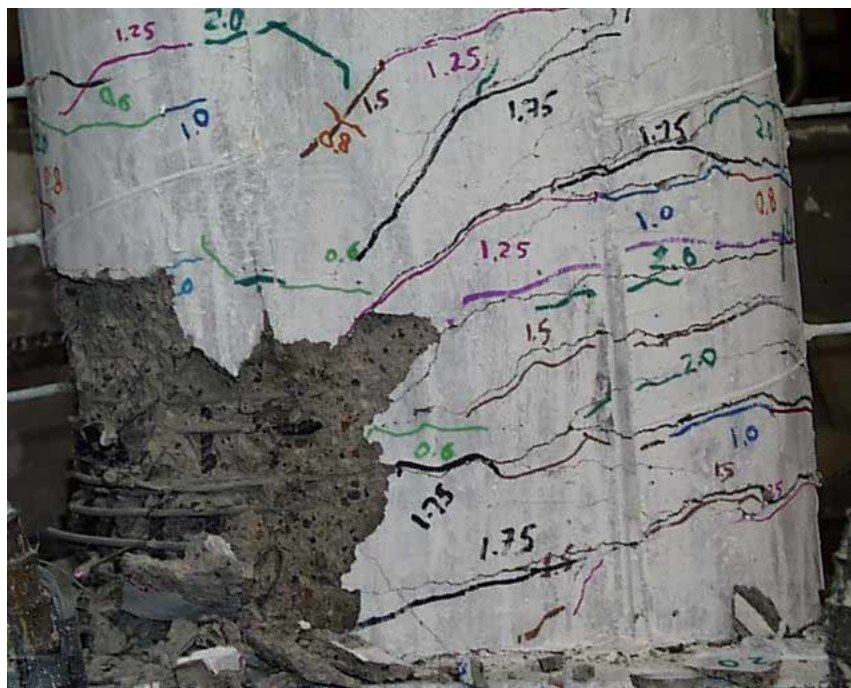


Figure 6. Specimens ISL1.5 after Collapse.

High Average Shear Stress Columns: ISH1.0, ISH1.25, ISH1.5 and ISH1.5T

During the first three runs, flexural cracks were observed in all specimens. A vertical crack located in the interlocking region along the height of the columns was visible at 0.4xSlymar (0.24g PGA) in specimen ISH1.5 (Figure 7). First shear cracks, located in the interlocking region, were formed in the specimens ISH1.0 and ISH1.5 at 0.5xSylmar and 0.6xSylmar, respectively. For specimens ISH1.25 and ISH1.5T shear cracks appeared at 0.75xSylmar. Localized small vertical cracks were observed in specimen ISH1.5T at 1.0xSylmar. After 1.0xSylmar, first spalling was observed in specimens ISH1.0 and ISH1.5, whereas in specimens ISH1.25 and ISH1.5T, first spalling was observed at 1.25xSylmar. The spirals were visible at 1.75xSylmar in specimen ISH1.25. Exposure of the longitudinal bar was observed at 1.75xSylmar in specimen ISH1.0, at 2.25xSylmar in specimen ISH1.25, at 1.5xSylmar in specimen ISH1.5 and at 2.0xSylmar in specimen ISH1.5T. The specimens ISH1.0 and ISH1.25 (Figures 8 and 9) failed in shear during 2.0xSylmar (1.21g PGA) at the bottom and 2.375xSylmar (1.44g PGA) at the top, respectively. Damage in the core was observed in specimens ISH1.5 and ISH1.5T after 2.125xSylmar. Buckling of the longitudinal bars was visible after 2.25xSylmar for specimen ISH1.5 and after 2.375xSylmar for specimen ISH1.5T. Specimen ISH1.5 and ISH1.5T (Figures 10 and 11) failed during 2.375xSylmar and 2.625xSylmar, respectively. Failure in specimen ISH1.5 was due to fracturing of the spirals and buckling of the longitudinal bars whereas in specimen ISH1.5T, it was due to fracturing of the spirals and one of the longitudinal bars.



Figure 7. Specimens ISH1.5 vertical crack

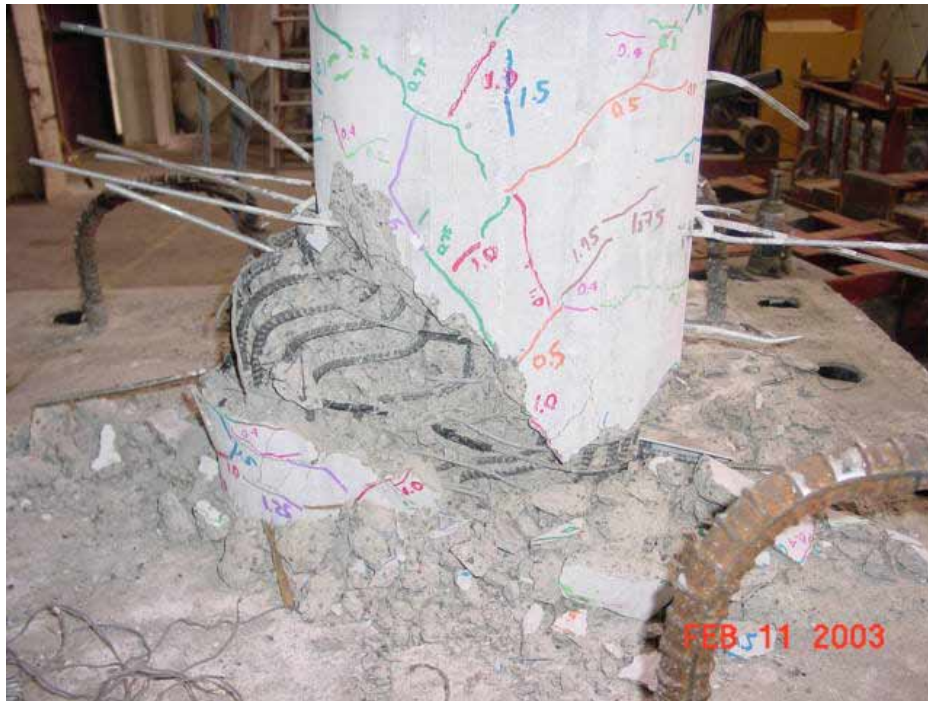


Figure 8. Specimens ISH1.0 after Collapse



Figure 9. Specimens ISH1.25 after Collapse



Figure 10. Specimens ISH1.5 after Collapse



Figure 11. Specimens ISH1.5T after Collapse

MEASURED PERFORMANCE

Low Average Shear Stress Columns: ISL1.0 AND ISL1.5

The measured hysteretic curves, for specimens ISL1.0 and ISL1.5, are shown in Figure 12 and 13, respectively. The maximum force reached in the specimen ISL1.0 was 169 kN (38 Kips) whereas in ISL1.5 was 180 kN (40 Kips). Specimens ISL1.0 and ISL1.5 had a maximum displacement of 161 mm (6.34 in) and 216 mm (8.52 in), respectively. The envelope curve and idealized elasto-plastic model, for the predominant direction of the motion, are plotted in Figure 12 for specimen ISL1.0 and Figure 13 for ISL1.5. The ultimate displacement of 188 mm (7.42 in) for ISL1.5 was taken as the corresponding displacement of 80% of the maximum force. Based on the elasto-plastic model ductility displacement capacity of 9.5 and 10.4 was achieved for the specimens ISL1.0 and ISL1.5, respectively. In addition, similar stiffnesses of 9634 kN/mm (55 Kips/in) for ISL1.0 and 9282 kN/mm (53 Kips/in) for ISL1.5 were calculated from the elasto-plastic model.

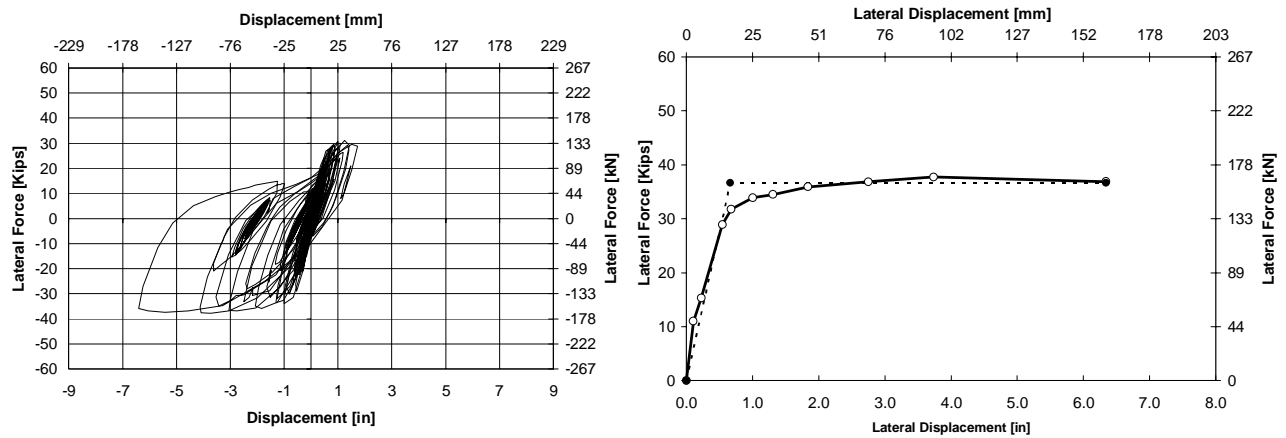


Figure 12. Hysteretic Curve and Envelope ISL1.0

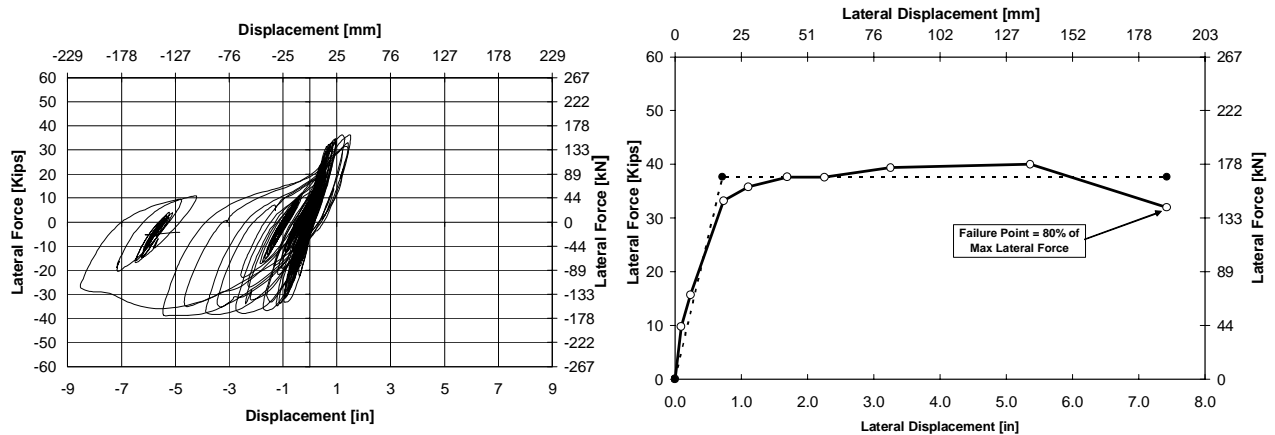


Figure 13. Hysteretic Curve and Envelope ISL1.5

High Average Shear Stress Columns: ISH1.0, ISH1.25, ISH1.5 and ISH1.5T

Figures 14, 15, 16 and 17 show the measured hysteretic curves and the envelope curves with idealized elasto-plastic models, for specimens ISH1.0, ISH1.25, ISH1.5 and ISH1.5T, respectively. The maximum force recorded in specimen ISH1.0 was 241 kN (54.25 Kips) and the maximum force for ISH1.25 was 251 kN (56.47 Kips). For specimens ISH1.5 and ISH1.5T the maximum force was 247 kN (55.56 Kips) and 251 kN (56.48 Kips), respectively. Maximum displacements of 108 mm (4.24 in), 105 mm (4.15 in), 128 mm (5.05 in) and 101 mm (4.0 in) were achieved in specimens ISH1.0, ISH1.25, ISH1.5 and ISH1.5T, respectively. For the envelope curves, the corresponding displacement of 80% of the maximum force was taken as the ultimate displacement in specimens ISH1.0, ISH1.25 and ISH1.5. According to the elasto-plastic models, ductility displacement capacities of 4.7, 5.0, 4.0 and 3.8 were achieved for the specimens ISH1.0, ISH1.25, ISH1.5 and ISH1.5T, respectively. Furthermore, stiffnesses of 10808 kN/mm (62 Kips/in), 10972 kN/mm (63 Kips/in), 6949 kN/mm (40 Kips/in) and 8810 kN/mm (50 Kips/mm) for specimens ISH1.0, ISH1.25, ISH1.5 and ISH1.5T were calculated from the elasto-plastic model.

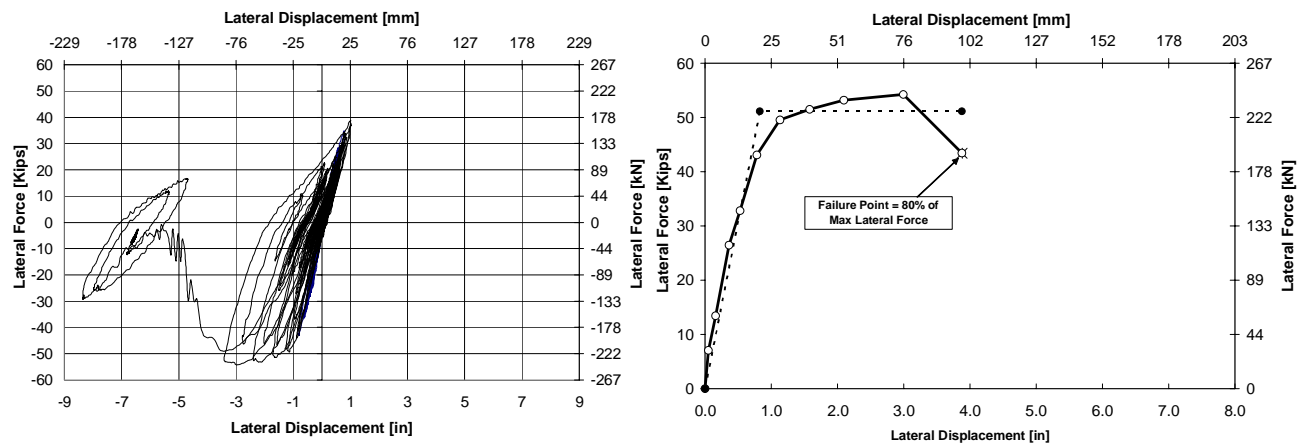


Figure 14. Hysteretic Curve and Envelope Specimen ISH1.0.

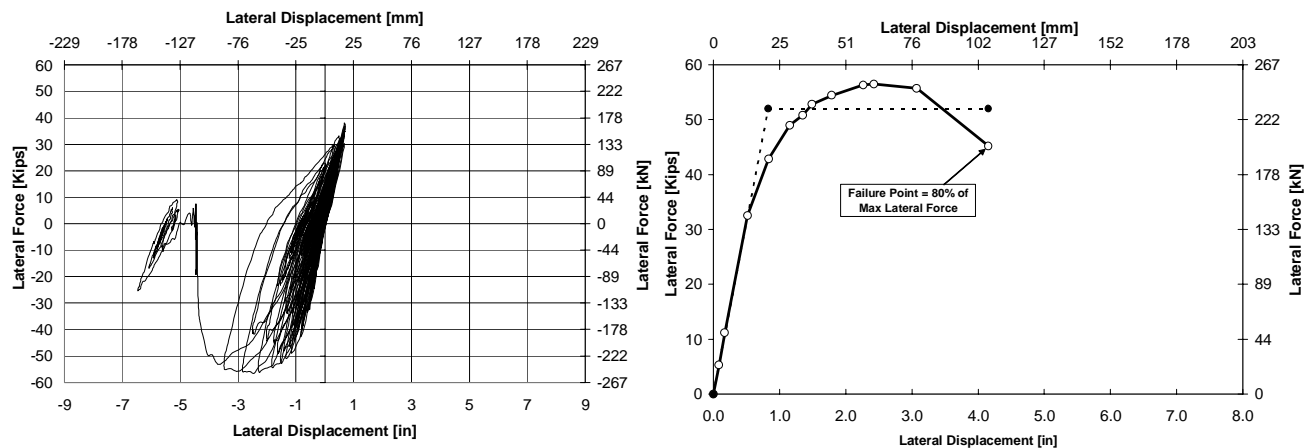


Figure 15. Hysteretic Curve and Envelope Specimen ISH1.25.

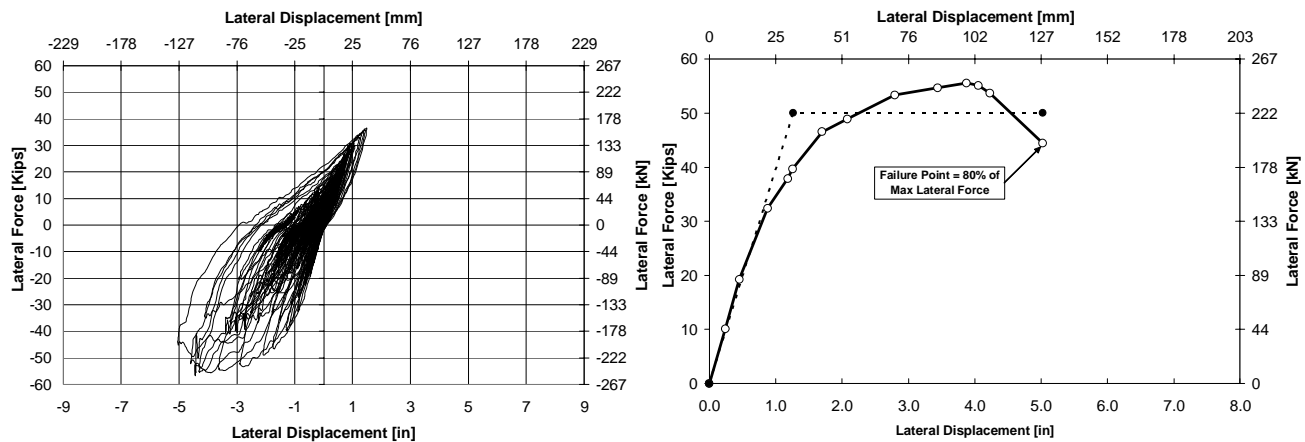


Figure 16. Hysteretic Curve and Envelope Specimen ISH1.5.

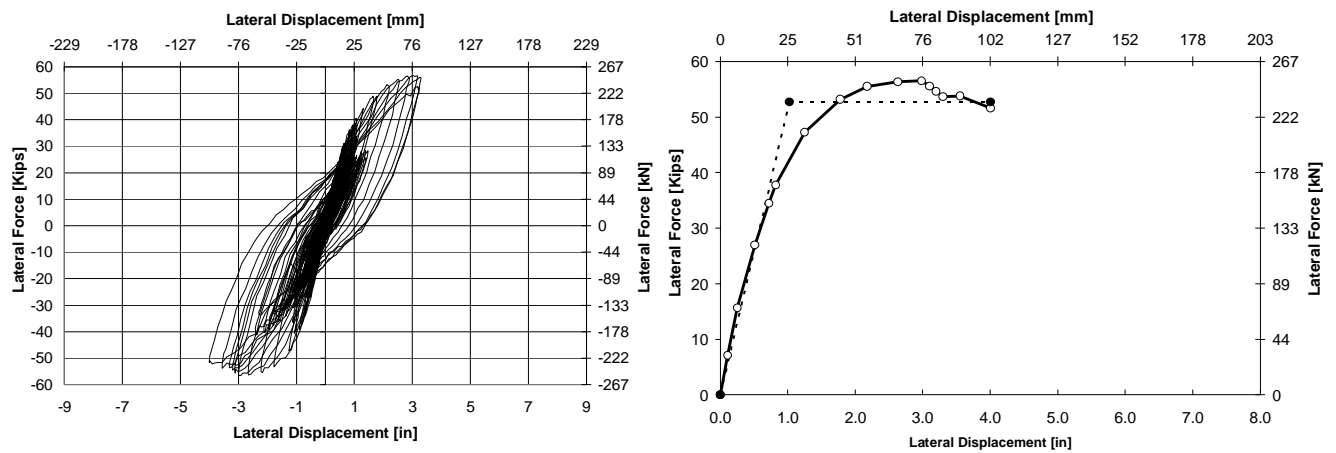


Figure 17. Hysteretic Curve and Envelope Specimen ISH1.5T.

A comparison of the predicted lateral force versus displacement and the elasto-plastic idealization of the experimental results are made in Table 2 and 3, for specimens with low and high average shear stress, respectively. The prediction of the lateral force was in good agreement with the experimental results. The yield displacement as well as the ultimate displacement was underestimated by the predicted displacement capacity.

Table 2. Comparison of SDC-Caltrans and experimental data low shear specimens

| Average Shear Stress/ $\sqrt{f'_c}$ MPa [psi] | d_i [R] | Force kN [Kips] | | Δy mm [in] | | Δu [in] | | μ | |
|--|-----------|-----------------|--------------|--------------------|--------------|-----------------|--------------|-----------------|--------------|
| | | SDC-99 Caltrans | Exp. Results | SDC-99 Caltrans | Exp. Results | SDC-99 Caltrans | Exp. Results | SDC-99 Caltrans | Exp. Results |
| 0.25 [3] | 1.0 | 153 [34] | 163 [37] | 10 [0.40] | 17 [0.67] | 43 [1.67] | 161 [6.34] | 4.2 | 9.5 |
| | 1.5 | 171 [38] | 168 [38] | 13 [0.49] | 18 [0.72] | 56 [2.19] | 188 [7.42] | 4.4 | 10.4 |

Table 3. Comparison of SDC-Caltrans and experimental data high shear specimens

| Average Shear Stress/ $\sqrt{f'_c}$ MPa [psi] | di [R] | Force kN [Kips] | | Δy mm [in] | | Δu [in] | | μ | |
|--|--------|-----------------|--------------|--------------------|--------------|-----------------|--------------|-----------------|--------------|
| | | SDC-99 Caltrans | Exp. Results | SDC-99 Caltrans | Exp. Results | SDC-99 Caltrans | Exp. Results | SDC-99 Caltrans | Exp. Results |
| 0.58 [7] | 1.0 | 202 [45] | 228 [51] | 6 [0.25] | 21 [0.83] | 27 [1.06] | 99 [3.88] | 4.2 | 4.7 |
| | 1.25 | 217 [49] | 231 [52] | 6 [0.22] | 21 [0.83] | 29 [1.16] | 106 [4.15] | 5.3 | 5.0 |
| | 1.5 | 199 [45] | 223 [50] | 10 [0.38] | 32 [1.26] | 38 [1.48] | 128 [5.02] | 3.9 | 4.0 |
| | 1.5T | 210 [47] | 235 [53] | 9 [0.35] | 27 [1.05] | 32 [1.25] | 102 [4.00] | 3.6 | 3.8 |

CONCLUSIONS

Based on the interpretation of the experimental results presented in this article the following conclusions were made for bridge columns with double interlocking spirals:

1. The seismic performance of two columns (ISL1.0 and ISL1.5) subjected to low average shear stress was similar and satisfactory. The measured displacement ductility capacity of 9.5 and 10.4 in columns ISL1.0 and ISL1.5 exceeded the target ductility of 5.
2. The larger distance between the centers of the spirals in ISL1.5 did not lead to excessive shear cracking or a reduction of the shear capacity, when the column is subjected to low level of shear forces. The Caltrans provision of allowing the distance to reach 1.5R is satisfactory at that low level of average shear forces.
3. The seismic performance of columns ISH1.0 and ISH1.25 subjected to high average shear stress was similar. The measured displacement ductility capacities for both specimens were in good agreement to the target ductility of 5.
4. Specimens ISH1.5 and ISH1.5T did not achieve the target displacement ductility capacities of 5 but exceeded the minimum specified displacement ductility capacity of 3, according to SDC [1].
5. Considerable reduction of displacement ductility capacities was obtained in the columns subjected to high average shear stress, compared to columns subjected to low average shear stress.
6. Vertical cracks were observed in the specimen ISH1.5 with high average shear stress at about 58 % of the maximum force. Horizontal cross ties connecting the hoops (ISH1.5T) reduce vertical cracks in the interlocking region.
7. In order to improve the correlation between experimental results and predicted values, a bond slip and shear deformation should be included in the calculation of the idealized yield displacement capacity. In addition, a modified or new equation for the equivalent analytical plastic hinge length should be developed for the calculation of the ultimate displacement.

ACKNOWLEDGEMENT

The research presented in this paper was sponsored by the California Department of Transportation. However, the opinions and conclusions reported in this paper are those of the authors only and do not necessarily reflect the views of the sponsor.

REFERENCES

1. Caltrans, 1999, Seismic Design Criteria, California Department of Transportation, Sacramento, California.
2. Tanaka, H., Park, R. "Seismic Design and Behavior of Reinforced Concrete Columns with Interlocking Spirals", ACI Structural Journal March-April 1993
3. Buckingham, G.C. "Tests of Concrete Bridge Columns with Interlocking Spirals Reinforcement", presented at the Transportation Research Board 72nd annual meeting, January 11-17, 1993.
4. Benzoni, G., Priestley, M.J.N., Seible, F. "Seismic Shear Strength of Columns with Interlocking Spiral Reinforcement", 12th World Conference on Earthquake Engineering, Auckland, New Zealand, 2000.
5. Mizugami, Y. "Efficiency of Lateral Reinforcement in interlocking Spirals Re-bar", presented at the 16th US-Japan Bridge Engineering Workshop, October 2-4, 2000.
6. SPMC, VER. 10. Moment-Curvature Analysis for Interlocking Spirals by Wehbe Nadim, Assistant Professor Of Civil Engineering, South Dakota State University, Brookings, July 2001.
7. RCShake, VER 2.31. Dynamic Time History Analysis for the UNR Shake Table and Mass Rig System by Patrick Laplace, Department of Civil Engineering, University of Nevada, Reno, July 2001.